A Novel Generation and Measurement Setup for the Characterization of MV Voltage Transformers From 9 kHz up to 150 kHz

Gabriella Crotti, Giovanni D'Avanzo, Antonio Delle Femine, *Member, IEEE*, Daniele Gallo, *Member, IEEE*, Domenico Giordano, *Member, IEEE*, Claudio Iodice, *Graduate Student Member, IEEE*, Carmine Landi, *Senior Member, IEEE*, Palma S. Letizia, Mario Luiso, *Member, IEEE*, and Paolo Mazza

***Abstract*— This article proposes a generation and measurement setup for the characterization of voltage transformer (VT), both inductive as well as low power voltage transformers (LPVTs) at power frequency and from 9 to 150 kHz with waveforms having amplitudes at medium voltage (MV) level. It involves the independent generation of the fundamental tone and of the high-frequency components to produce the desired distorted test waveform. The generation of the fundamental frequency component, in MV amplitude range, is obtained by means of a step-up VT, whereas the high-frequency components are generated through a series-connected voltage amplifier. As regards the measuring stage, the fundamental tone is measured through a commercial divider. Instead, high-frequency tones are measured through a reference device, operating in the range [9, 150] kHz, specifically designed, realized, and characterized. As an application, the characterization of two commercial VTs, an inductive VT and a LPVT, are presented.**

***Index Terms*— High-frequency components, instrument transformer (IT), low-power voltage transformer (LPVT), medium voltage (MV), power system measurements, reference voltage divider, switching power converter, voltage transformer (VT).**

I. Introduction

SOCIETY'S increasing use of switching devices (inverters, bulky power electronic converters, and active filters) both as loads as well as part of generators, especially for renewable energy sources, has driven a consequent proliferation of conducted disturbances on grid voltage and current, also at medium voltage (MV) level, up to hundreds of kilohertz, due to the harmonics of the switching frequency.

For instance, the conducted emissions of new switching devices can interfere with power line communication (PLC). PLC is a widely used communication technique over electrical grids to fulfill vital operations such as control and automation [1]; this interference degrades the quality of the delivered information and possible failures of vital grid operations can occur [2], [3], [4]. High-frequency emissions from one device (both a load or a generator, including high-power converters) can easily couple with other devices, causing interference to the control system of the other devices, with possible consequent malfunctions or even complete failure. Moreover, these emissions increase the root mean square (RMS) value of the current that, along with a pronounced skin effect, causes temperature increase and, consequently, accelerated aging and reduced useful life of components.

Recently, power converters, e.g., DC/DC (direct current), AC/DC (alternating current), and AC/AC, which make use of new-generation switching components, e.g., silicon carbide (SiC) metal oxide semiconductor field effect transistors (MOSFETs) [5], [6] allowing for increased switching frequencies, can be directly connected to MV power systems. This fact opens, also for MV grids, measurement needs that low-voltage (LV) grids already experienced [7], [8], [9], [10]. These needs, in turn, ask for new and improved performance, in terms of accuracy and wide frequency range. Unavoidably, the same requirements apply to instrument transformers (ITs), as they are the first element of every voltage and current measuring chain, in practically all power system applications.

From the point of view of standardization about ITs, the in–force standards covering the accuracy of ITs are the those of IEC 61869 family [11]. They are focused on ITs for MV and high-voltage (HV) grids and the part 1 [12] gives an extension of accuracy requirements up to 500 kHz. However, they do not give indications on measurement methods, test procedures, possible reference instrumentation, or uncertainty evaluation at frequencies above the 13th harmonic order. In this way, they leave to the manufacturer, or to the calibration laboratory, a complete arbitrariness on how to evaluate the fulfillment of the prescribed accuracy requirement above power frequency, leaving, in turn, the final user in the impossibility to validate the performance of products.

Manuscript received 10 April 2024; revised 14 June 2024; accepted 24 June 2024. Date of publication 28 August 2024; date of current version 9 September 2024. This work was supported in part by MUR Progetti di Ricerca di Rilevante Interesse Nazionale (PRIN) Bando 2022 under Project 2022FLWXTA "EMIslands", in part by MUR Progetti di Ricerca di Rilevante Interesse Nazionale (PRIN)-PRIN 2022PNRR under Project P2022XL9NX "MERSIS", in part by the European Partnership on Metrology (EPM) under Project 22NRM06 ADMIT, and in part by the European Partnership on Metrology, co-financed by the European Union's Horizon Europe Research and Innovation Programme and the Participating States under Project 22NRM06 ADMIT. The Associate Editor coordinating the review process was Dr. He Wen. *(Corresponding author: Mario Luiso.)*

Gabriella Crotti, Domenico Giordano, and Palma S. Letizia are with the Istituto Nazionale di Ricerca Metrologica, 10135 Turin, Italy (e-mail: g.crotti@inrim.it; d.giordano@inrim.it; p.letizia@inrim.it).

Giovanni D'Avanzo and Paolo Mazza are with Ricerca sul Sistema Energetico S.p.A., 20134 Milan, Italy (e-mail: giovanni.davanzo@rse-web.it; paolo.mazza@rse-web.it).

Antonio Delle Femine, Daniele Gallo, Claudio Iodice, Carmine Landi, and Mario Luiso are with the Dipartimento di Ingegneria, Università degli Studi della Campania "Luigi Vanvitelli," 81031 Aversa, Italy (e-mail: antonio.dellefemine@unicampania.it; daniele.gallo@unicampania.it; claudio.iodice@unicampania.it; carmine.landi@unicampania.it; mario.luiso@unicampania.it).

Digital Object Identifier 10.1109/TIM.2024.3427768

The activity presented here is developed according to the framework of the European Partnership in Metrology (EPM) 22NRM06 "ADMIT" [13], which aims to establish suitable parameters for the definition of the accuracy of voltage and current transformers (VTs and CTs), and the related measurement instrumentation, in the frequency range from 9 kHz up to 150 kHz. A nonexhaustive list of the activities that will be carried out within this project is: definition of realistic waveforms, accuracy parameters, and related procedures for the performance evaluation of ITs, development of new systems for the generation of AC (50/60 Hz) or DC voltages (up to 36 kV) and currents (up to 2 kA) with spectral components of reduced amplitudes up to 150 kHz, and development of reference MV voltage and current sensors up to 150 kHz. As a starting point, this article deals with the design and the implementation of a novel generation and measurement setup that allows for characterizing VTs for AC grids up to 3 kV, at 50/60 Hz and in the frequency range from 9 kHz up to 150 kHz. It is worth pointing out that the range of frequencies of interest in the activities carried out and here presented excludes frequencies lower than 9 kHz. In fact, for this frequency range, solutions have already been developed and validated in the framework of other European research projects, such as Future Grid II [14], [15] and IT4PQ [16], [17], and in general, they have been addressed and presented in the scientific literature [18], [19], [20], [21]. The reference setups and test procedures proposed for the ITs characterization up to 9 kHz represent a starting point in the study of new solutions to cover the frequency range up to 150 kHz but, from both the generation and measurement points of view, new issues arise and require further investigations.

This article is an extended version of the conference paper [22]: it presents a possible architecture of a generation system for the frequencies of interest. Following it, this article examines the issues and suggests a possible solution related to the generation of high-frequency tones superimposed to the MV component at power frequency, when this is generated using a step-up transformer. Moreover, a novel reference device for measuring voltage components in the range from 9 kHz up to 150 kHz, when also a MV component at power frequency is present in the test waveforms, is designed, built, and characterized. As an application, the proposed generation and measurement setup is used to determine the frequency behavior of a low-power VT (LPVT) and an inductive VT.

The structure of the paper is as follows. Section II presents a literature review of the VTs characterization up to 150 kHz. Section III presents the design of the reference generation and measurement setup. Section IV shows the characterization of a reference device. Section V introduces the measurement model and the associated uncertainty budget related to the evaluation of the frequency behavior of a VT. Section VI shows the characterization of two commercial VTs, a LPVT and an inductive VT. At last, Section VI draws the conclusions.

II. Review of Literature About the Characterization of VTs Up to 150 kHz

As mentioned in Section I, it is essential to highlight that the range from 9 kHz up to 150 kHz is an extension of the range considered in previous European research projects, that aimed at investigating the IT performances up to 9 kHz. The characterization methods, test waveforms, and measurement setups for the verification of the metrological performance of ITs up to 9 kHz are studied in [23], [24], [25], [26], [27], [28], [29], [30], [31], [32], [33], [34], [35], [36], [37], [38], [39], [40]; some of these papers are co-authored by some authors of the present paper. In the literature, it is quite widely recognized that the measurement of the frequency behavior of the ITs should be performed by applying waveforms composed of a fundamental tone (DC or AC 50/60 Hz) and one or more spectral tones with reduced amplitude. These kinds of tests are generally referred to as FH1 (Fundamental plus 1 Harmonic) and FHN (Fundamental plus N Harmonic components). However, to the best of the authors' knowledge, the investigated frequency range has been confined to 10 kHz, with only a few papers that investigate beyond this frequency. However, those that explored higher frequencies remain restricted to a quite low-frequency range, e.g., 20 kHz, as in [38]. Currently, to the best of the authors' knowledge, National Metrology Institutes (NMIs) are able to characterize the VTs with FH1 or FHN waveforms having fundamental components up to some tens of kilovolt and other spectral components with frequency up to 9 kHz and reduced amplitude; instead they are able to characterize the VTs up to 150 kHz and 100 V with sine waves. The main reason for those limitations to frequency and amplitude ranges is due to the fact that no voltage reference measuring devices nor generation and measurement setups that can work simultaneously with amplitude in the MV range and up to 150 kHz are currently available.

One field of application with some common points with this article's research topic is the measurement of high-voltage pulses [30]. The common points regard essentially the voltage range (up to tens of kilovolt, or even more) and the frequency range (from DC up to hundreds of kilohertz or more). However, critical differences between these two topics make the HV pulse measurement methodologies not directly applicable to the characterization of ITs, intended for power system applications, up to 150 kHz. The main reason is the great difference between the waveforms involved in these two applications. In the case of HV pulse measurement, they are short square or exponential pulses (in the order of $0.1 \div 10$ μs), whereas in the second case, they are composed of a sine wave, at fundamental frequency, with superimposed other high-frequency sine waves with reduced amplitudes.

In conclusion, to the best of the authors' knowledge, there are no solutions already developed for the metrological characterization of MV VTs up to 150 kHz, for what concerns reference devices and generation and measurement setup.

III. Design of the Reference Generation and Measurement Setup

The solution here adopted for the VT characterization is based on the comparison of the outputs of a reference VT and of a VT under test by means of a comparator, under waveforms representative of actual power system waveforms [21]. Both the comparator as well as the reference VT should have sufficient accuracy in the investigated frequency range. As regards the generation, currently, there are no

directly applicable solutions for the realization of generation systems capable of meeting the two necessary requirements for testing VT under actual conditions. These requirements include high-voltage levels at fundamental frequency and a frequency bandwidth extending up to 150 kHz, with the aim of generating hundreds of volt within this frequency range. Moreover, no reference device can be currently characterized under waveforms having a MV fundamental tone and LV frequency components from 9 to 150 kHz. In this context, two solutions are discussed below, one related to the generation system and one to the reference device, whereas analyzing and addressing the associated issues. For the sake of simplicity and without loss of generality, in the rest of the paper, reference will be made to 50 Hz as the used fundamental frequency.

It is worth to underline that the indications discussed in the following, for the design of the generation and measuring setup, are general and do not depend on the specific implementation adopted in this article. Also, the operating voltage level can be easily extended, by using the proper generation and measurement devices and the proper safety measures. Therefore, following the proposed architecture and adapting the design parameters to the specific characterization needs, it is possible to obtain an implementation of a generation and measurement setup suitable for the specific scope.

A. Architecture of the Proposed Generation and Measurement Setup

In Fig. 1(a), the general block scheme of the proposed novel setup is presented, whereas a picture is shown in Fig. 1(b). The setup has been realized at the University of Campania "Luigi Vanvitelli" and used in a temperature-controlled room. It overcomes the generation and measurement limits outlined in Section III. As regards the generation, as mentioned in Section II, the most commonly used test waveforms for the VT frequency characterization are composed of fundamental tone at the rated frequency and amplitude and one or more superimposed tones at different frequencies and with reduced amplitudes. The proposed solution involves the independent generation of the fundamental tone and of the high-frequency components to produce the desired distorted test waveform.

According to a commonly used practice in calibration laboratories (but also at NMI level), the generation of fundamental frequency components up to hundreds of kilovolt can be obtained by means of step-up voltage transformers (SUTs). Similarly, the proposed architecture generates the fundamental component using an arbitrary waveform generator (AWG1), a low-voltage and low-frequency amplifier (LFA), and a SUT. Due to its intrinsic galvanic insulation, this method allows for the generation of a voltage waveform with respect to a desired reference potential. It is important to underline that the desired reference potential should not necessarily be the Earth potential or the reference potential of the rest of the circuit, thanks to the galvanic insulation of the SUT. Therefore, the secondary winding of the SUT can be easily series connected with another generation system as well depicted in Fig. 1(c).

Considering that the frequency components have an amplitude lower than fundamental components, up to 3% [21], they can be generated using AWG2 coupled with a high-frequency

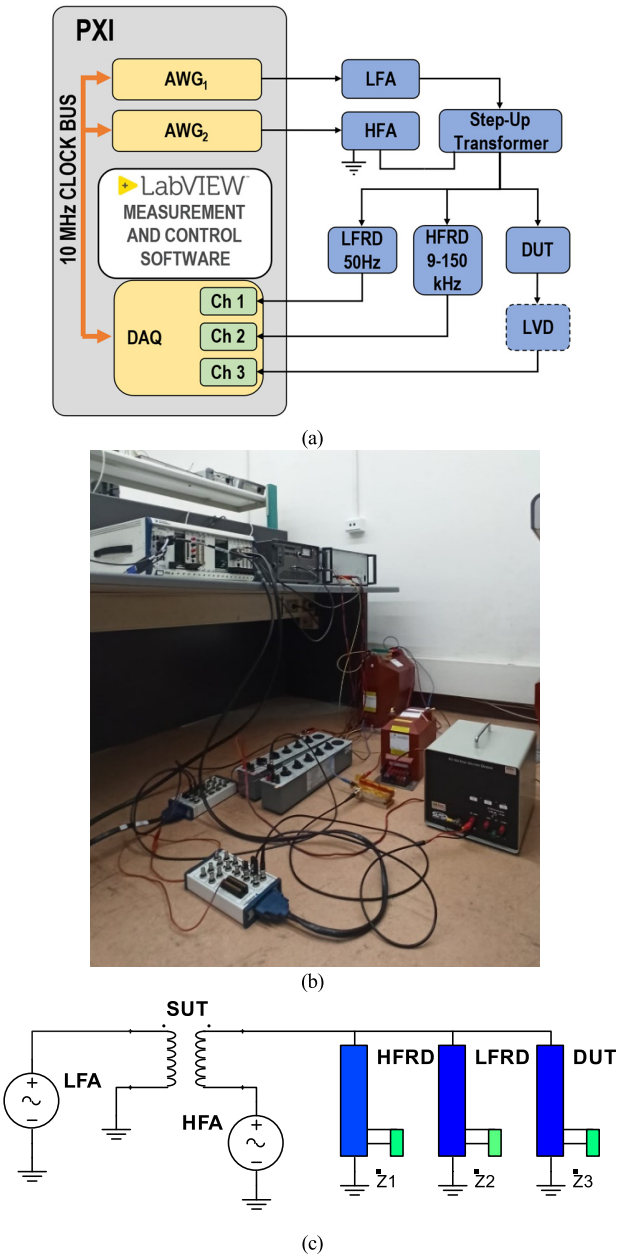

Fig. 1. (a) Basic block scheme, (b) picture, and (c) circuit diagram of the proposed generation and measurement setup arranged at University of Campania.

amplifier (HFA). Thus, the distorted test waveforms can be obtained by simply using the SUT and HFA connected in series to superimpose the frequency components in the range [9, 150] kHz to the MV component at 50 Hz.

As regards the measurement section, two different reference transducers are used, one [low-frequency reference device (LFRD), calibrated at INRIM] [39], [41] for the measurement of the power frequency component at MV level and the other [high-frequency reference device (HFRD)] for the measurement of the high-frequency components, characterized by amplitudes in the range up to hundreds of volt. It is worth noting that one of the main goals of the ADMIT project [13] is the design, the realization, and the characterization of reference sensors operating in the frequency range [9, 150] kHz and capable to work at MV amplitude levels.

TABLE I
MAIN SPECIFICATIONS OF THE SETUP COMPONENTS

NAME	MAIN FEATURES
AWGs	National Instruments (NI) PCI eXtension for Instrumentation (PXI) 5422, 16-bit, variable output gain, ± 12 V output range, 200 MHz maximum sampling rate, and 256 MB of onboard memory.
LFA	Voltage amplifier, ± 75 V, ± 20 A, 1 kW, DC – 100 kHz
SUT	Step-Up Voltage Transformer, 100 V / 24 kV
HFA	Voltage amplifier, ± 150 V, 200 VA, DC – 500 kHz.
DAQ	Data acquisition module NI PXIe-6124, ±10 V, 16 bit, maximum sampling rate of 4 MHz, input resistance >100 GΩ with parallel 10 pF.
LFRD	Commercial resistive-capacitive divider, 10 / 10 kV/V, uncertainty of 0.01% and 100 µrad @ 50 Hz (level of confidence 95 %)
LVD	Commercial resistive divider, 18.5 V/V, uncertainty of 0.01% and 100 µrad @ 50 Hz (level of confidence 95 %)

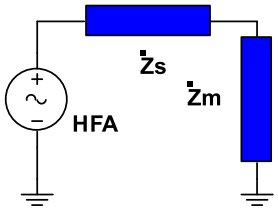

Fig. 2. Equivalent circuit of the setup in the range from 9 kHz up to 150 kHz.

As regard the acquisition section, the comparator is realized by using a data acquisition (DAQ) module that acquires the outputs of the device under test, of LFRD and of HFRD. Gain and offset of the adopted DAQ have been determined at INRIM. The DAQ module is installed in a PXI chassis along with the AWGs; the 10 MHz PXI clock is used as a reference clock for the AWGs phase-locked loop (PLL) circuitry. The time base of AWG1 provides also the sampling clock for the digitizer; this allows obtaining coherent sampling, thus avoiding spectral leakage.

Moreover, in Fig. 1(c), the impedances $\dot{Z}_1$, $\dot{Z}_2$, and $\dot{Z}_3$ (green color) are the input impedance of the DAQ channels. Moreover, if the DUT output voltage is too high to be directly acquired by the DAQ (as in the case of inductive VTs), a LV divider (LVD) is used [see Fig. 1(a)]. This divider can be characterized by NMIs at voltage levels in the range of hundreds of volt up to 150 kHz.

The main specifications of the various devices used to implement the described setup are summarized in Table I.

B. Issues in the Generation Circuit

The series connection of the two generators discussed in Section III-A presents some issues that must be addressed in order to make this architecture suitable for the scope at hand.

First of all, according to the equivalent circuit of a voltage transformer (VT) [42], the equivalent impedance $\dot{Z}_s(f)$ of the secondary winding, in the frequency range [9, 150] kHz, is mainly inductive and increases with frequency. Therefore, in the frequency range [9, 150] kHz, the equivalent circuit (shown in Fig. 2) of the measurement setup is constituted by the HFA and its load, that is the series connection of $\dot{Z}_s(f)$ and $\dot{Z}_m(f)$, that, in turns, is the equivalent impedance resulting from the parallel of the input impedances of DUT, LFRD, and HFRD.

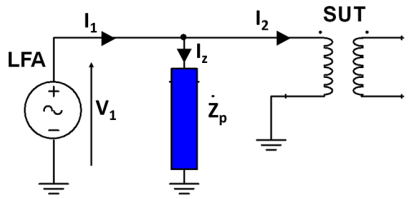

Fig. 3. Equivalent circuit of the setup at the primary side of SUT.

Looking at the Fig. 2, it can be seen that the output voltage of HFA is divided among $\dot{Z}_s(f)$ and $\dot{Z}_m(f)$. The voltage drop across $\dot{Z}_s(f)$, that is undesired, increases with frequency, making thus the portion of voltage across $\dot{Z}_m(f)$ smaller and smaller. To avoid this issue, it is possible to add a capacitor C_s in parallel to the secondary winding of SUT in order to drastically reduce the voltage drop across $\dot{Z}_s(f)$.

However, the insertion of C_s at the SUT output increases the load of LFA. In fact, the equivalent impedance $\dot{Z}_s(f)$ (including now C_s), transferred at the primary side of SUT, must be sufficiently high, at 50 Hz, to stay within the current limit of LFA (LFA generates voltage and current at 50 Hz). Since the rated transformation ratio of SUT is $k = (N_p/N_s)$, where N_p (N_s) is the number of turns at primary (secondary) winding, the load impedance of LFA is $\dot{Z}_p(50) = k^2\dot{Z}_s(50)$. In the case of SUT, N_s is higher than N_p and then k is lower than 1. Therefore, the magnitude Z_p of $\dot{Z}_p$ is lower than Z_s. To calculate the maximum value of C_s, the current of the primary winding of SUT must be considered. For sake of clarity, Fig. 3 shows the circuit for the calculation of $C_{s,\max}$. The current I_1 is the maximum LFA output current, which divides in I_2 and I_z, which are, respectively, the magnitudes of the current that flows in the primary winding of SUT and of the current that flows in $\dot{Z}_p$. I_2 depends on the load of the SUT. However, generally, the load impedance of SUT is high; therefore, the I_2 can be assumed to be the magnetizing current of SUT. Therefore, the maximum value of C_s is calculated by the following equation:

$$C_{s,\max} = \frac{I_z}{2\pi f_1 V_1} \tag{1}$$

where V_1 and f_1 are, respectively, the maximum magnitude of the fundamental voltage phasor and its frequency and I_z is the difference between I_1 and I_2. For the case at hand, $C_{s,\max}$ is equal to 50 nF.

As regards the current limit of HFA, the magnitude of the equivalent series impedance of $\dot{Z}_s(f)$ and $\dot{Z}_m(f)$ must be sufficiently high to stay within the current limitation of HFA in the frequency range [9, 150] kHz. This condition generally holds, since the input impedance of the VTs designed for MV applications is generally high. However, it is worth noting that a check against the limitations of the HFA generator must be done before the execution of the tests.

C. Design of a Reference Device in the Range 9–150 kHz

As written in Section III, a novel reference device (HFRD) was specifically developed for the characterization of VTs in the frequency range [9, 150] kHz when also a MV tone

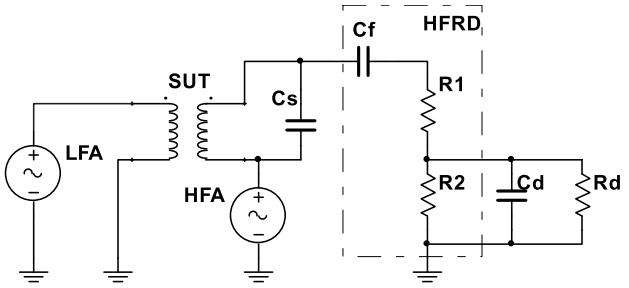

Fig. 4. Simplified circuit diagram of the proposed generation and measurement setup.

at the 50 Hz is included into the test waveform. Currently, some NMIs offer calibration services of voltage measuring devices in the frequency range [9, 150] kHz, but they are limited to voltage levels up to 100 V and make use of only sine waves. To overcome this limitation, the proposed HFRD has a high-pass filtering behavior, with a cutoff frequency of 5 kHz in order to attenuate in a significant way the amplitude of the 50 Hz component at MV level. Additionally, HFRD has to exhibit a quite flat response in the [9, 150] kHz range with a proper scale factor (SF) to ensure the reduction of tone amplitudes to levels compatible with the input stage of the acquisition system, typically within the range of ± 10 V. In the design of such a device, it is also necessary to consider the contribution of the impedance (typically a resistance in parallel with a capacitance) introduced by the input circuit of the acquisition system.

As a result, considering the resistances and the capacitances required to implement HFRD, those introduced by the acquisition system and the capacitance introduced in parallel to the step-up transformer, a device with a bandpass behavior is obtained.

The simplified circuit diagram of HFRD is provided in Fig. 4, where also the generation section is reported. In particular.

1) C_s is the capacitance parallel connected to the SUT, as discussed in Section III-B.
2) C_f is the HFRD capacitance.
3) R_1 and R_2 are the two resistances implementing the resistive part of the HFRD filter and, at the same time, the resistive voltage divider with a fixed SF.
4) C_d and R_d represent the input capacitance and resistance of the acquisition system.

In the case under analysis, R_d exceeds 100 GΩ, and thus it can be neglected, C_d is about 400 pF (including also the capacitance of the connection box and of the cable that connects it to the board) and R_1 is selected almost equal to $76 \times R_2$ to achieve a SF equal to about 77 V/V. By defining R_{tot} as the series of R_1 and R_2 and C_{tot} as the series of C_s and C_f, the transfer function of HFRD can be written as

$$W(s) = \frac{sR_2C_sC_f(1/C_f + C_s)}{\left(1 + sR_{\text{tot}}C_{\text{tot}} + sR_2C_d + s^2R_1R_2C_{\text{tot}}C_d\right)}. \quad (2)$$

This transfer function is characterized by one zero in $s = 0$ and, by approximating $R_{\text{tot}} \approx R_1$, two poles, having the associated time constants equal to $\tau_{p,1} = R_{\text{tot}}C_{\text{tot}}$ and $\tau_{p,2} = R_2C_d$.

TABLE II
REFERENCE FILTER PARAMETERS

Parameter	Value
C_F	275 pF
Maximum capacitor voltage	4 kV (AC voltage)
R_1	114.3 kΩ
R_2	1.5 kΩ
Bandpass gain	$\approx 1/80$
f_{cutoff}	≈ 5 kHz

Considering that the value of C_d is fixed and it depends on the acquisition system and that the value of C_s is set to meet the generation requirements explained in Section III-B, C_f, R_1, and R_2 represent the only quantities that can be suitably selected to meet the design requirements. In this specific case, they are chosen as reported in Table II, where also the cutoff frequency and the bandpass gain are provided.

D. Linear and Nonlinear Parasitic Effects of HFRD Components

Generally speaking, the resistors and the capacitors of HFRD can present linear and nonlinear parasitic effects. For instance, the capacitive coupling (in the air) of the resistor terminals or the linear losses inside the capacitors can be considered linear effects; instead, the dependences of the resistance and of the capacitance on the amplitude of the applied voltages can be considered nonlinear effects. Therefore, before the realization of HFRD, every single component was subjected to various kind of tests in order to quantify these effects.

The linear effects were quantified by analyzing every single component through the Agilent (now Keysight) E4980A precision LCR meter, from 9 kHz up to 150 kHz. It was found that the best model for the resistors is a parallel connection of a resistance and of a capacitance; the parasitic capacitances are in the order $\sim$100 fF for resistances in the order $\sim$1–10 kΩ. Instead, the best model for the capacitors is a series connection of a resistance and of a capacitance; the parasitic resistances are in the order $\sim$0.1 Ω for capacitances in the order $\sim$100 pF. Obviously, the presence of such linear parasitic effects alters the frequency behavior of the components, making Fig. 4 and (2) be only approximated versions of, respectively, the circuit diagram and the transfer function of HFRD. However, the circuit diagram shown in Fig. 4 was numerically simulated, as it is and by including the measured linear parasitic effects. The maximum deviation between the magnitudes of the two simulated frequency responses was found lower than 0.25%. For this reason, in order to not confuse the reader, Fig. 4 and (2) do not include the linear parasitic effects. It is worth to underline that this decision does not affect the accuracy of the results shown in the rest of the article, that remain rigorous. In fact, although Fig. 4 and (2) neglect these effects, they are present in the physical realization of HFRD; thus, they are included in the frequency behavior measured in Section IV-A and treated as systematic effects, with the related measurement uncertainty, in the tests shown in Section VI. As regards the possible temperature dependence of resistors and capacitors, as it is specified in Section III-A, the used laboratory has

a temperature control system. Therefore, no temperature-dependent variations are expected.

For what concerns the nonlinear parasitic effects of both resistors as well capacitors, they are linked to the slight nonlinear behavior of the dielectric materials [43], [44], used for the internal insulation of the capacitors and as covers for the resistors. For the case at hand, the electrical properties of the dielectric material mainly depend on the RMS amplitude of the electric field inside the material, that is on the RMS amplitude of the voltage applied to the component (i.e., the resistor or the capacitor) [45], [46].

Since the modeling of nonlinear phenomena inside the electric components, like resistors and capacitors, is not the focus of the article, these phenomena are not considered in Fig. 4 and (2). Instead, the impact of these effects on the HFRD performance and the associated uncertainty are accurately evaluated from an experimental point of view and the obtained results are discussed in Section IV-C.

IV. Characterization of the Reference Device

The metrological characterization of the proposed device (HFRD) should be performed in the real operating conditions, that is with waveforms composed by a 50 Hz tone at MV level and one or more frequency components, with lower amplitude, in the range of [9, 150] kHz. However, this implies the necessity to have a reference device, to determine the metrological performance of HFRD. As highlighted in Section III, currently, to the best of the authors' knowledge, such a reference device is not available on the market nor at NMI level. This is why HFRD was developed.

Therefore, since in the frequency range [9, 150] kHz reference measurement instrumentation and procedures are available up to 100 V, the frequency behavior of the proposed device has been measured at LV level. Some physical considerations can be made to justify this approach. HFRD is a passive device, made exclusively with resistors and capacitors, that have, at least nominally, a linear behavior. Moreover, no resins or other insulation materials, with a possible nonlinear behavior, were used in the realization of HFRD. In addition, due to its high-pass frequency behavior, the 50 Hz component at MV level is strongly attenuated; it mostly drops across the input capacitor of HFRD and just a residual part drops across the output resistive divider. It follows that: HFRD resistors always work at voltage levels in the order of tens of volt and their dissipated power at the maximum voltage is just a little fraction (lower than 0.1%) of their power ratings.

Regarding the linear parasitic effects (see Section III-D), since they do not depend on the applied voltage, their presence is accurately accounted when the HFRD frequency behavior is measured at LV.

Following these considerations, the HFRD frequency behavior has been measured at 7 V in the range [9, 150] kHz. Then, in order to consider possible dependency from the amplitude level, the ratio and phase errors at 50 Hz were measured at various amplitudes. Similar procedures, up to about 10 kHz, are commonly used by NMIs [18], [47]. The nonlinear parasitic effects (Section III-D) are instead accounted by executing specific tests on every single HFRD component, as shown in Section IV-C, and included in the uncertainty budget.

The measurement results are obtained by performing a discrete Fourier transform (DFT) over ten cycles of the fundamental component as suggested by the international standards [48], [49]. For each measurement, 31 iterations have been performed to evaluate the repeatability and stability according to GUM [51].

The SF and the phase error of HFRD are obtained as in the following equations:

$$\mathrm{SF}_R(f) = \frac{V_p(f)}{V_s(f)} \tag{3}$$

$$\Delta\varphi_R(f) = \varphi_s(f) - \varphi_p(f) \tag{4}$$

where

$V_\mathrm{p}(f)$ and $V_\mathrm{s}(f)$ are the RMS values of the primary and secondary voltages at frequency f;

$\varphi_p(f)$ and $\varphi_s(f)$ are the phase angles of the primary and secondary voltages at frequency f.

A. Low-Voltage Frequency Characterization

In this test, HFRD was supplied directly by AWG1 and two DAQ channels are used to acquire the outputs of AWG1 and of HFRD. Fig. 5(a) [Fig. 5(b)] shows the measured SF (phase error) of HFRD in the range [50 Hz, 150 kHz], obtained by means of a frequency sweep with sinusoidal waveforms, having amplitude of 7 V, and according to (3) and (4). The initial high-pass behavior, with a cut-off frequency of about 5 kHz, is clearly visible. Focusing on the high-frequency range, a low-pass trend, due to the parallel input capacitance of the comparator, that follows the nominal high-pass behavior and becomes effective from about 50 kHz, can be observed. Indeed, the insets in Fig. 5(a) and (b) show that, for frequency range from 50 kHz up to 150 kHz, the SF slightly raises, and the phase error drops below zero.

The uncertainties associated with SF_R ($\Delta\varphi_R$) have two contributions: the ratio (phase) error between the two DAQ channels (evaluated through a type B approach [51]) and the repeatability and stability (evaluated through a type A approach [51]). Nevertheless, the contribution due to DAQ channels is negligible with respect to the other contribution, especially at high frequency.

B. Voltage Dependence at Power Frequency

As described in Section IV, due to the possible voltage dependence of HFRD capacitor, possible deviations of HFRD behavior, when it is used with an input voltage in the MV range rather than in the LV range, can occur. Therefore, in order to account for these possible deviations, HFRD has been tested at 50 Hz with increasing amplitudes from 10% to 120% of the rated voltage of the generation system. In this test, done at 50 Hz, LFRD was used as reference device.

Fig. 6 shows the SF and the phase error deviations, at fundamental frequency and at different voltage amplitudes, with respect to the values obtained in the LV frequency characterization (see Section IV-A). It can be observed that the SF

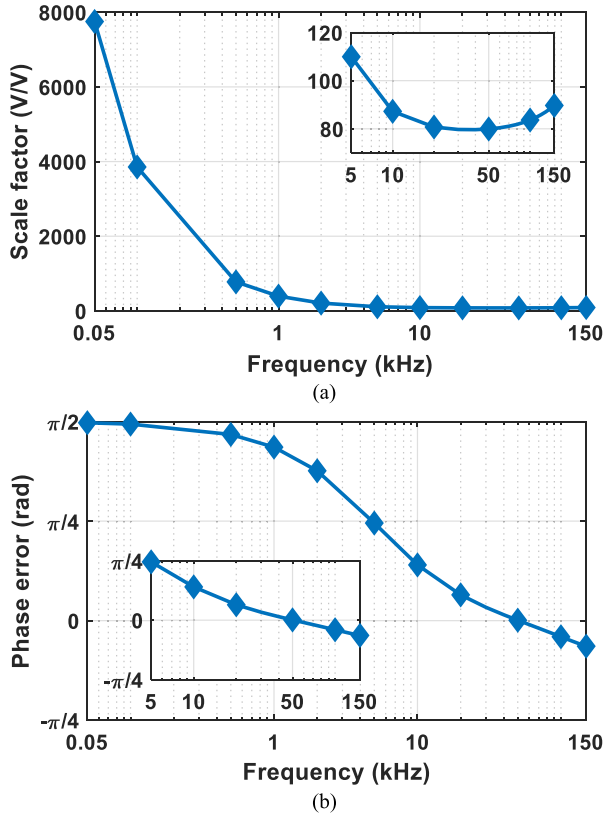

Fig. 5. (a) Frequency behavior of SF and (b) phase error of HFRD.

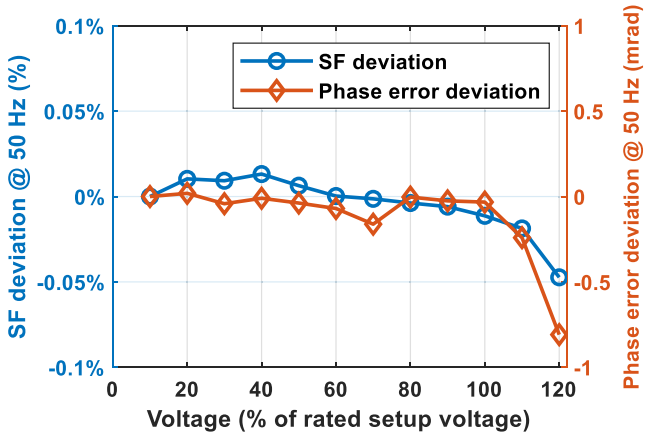

Fig. 6. SF and phase error deviation, with respect to the value measured at 7 V, at fundamental frequency versus the percentage of rated setup voltage.

(phase error) deviation is lower than 0.05% (within 0.8 mrad). These deviations of SF and phase error are included in the uncertainty associated with HFRD.

C. Impact of Nonlinear Parasitic Effects of HFRD Resistors and Capacitors

In this section, results related to the quantification of nonlinear parasitic effects of one single resistor and one single capacitor of HFRD are shown; similar results are obtained for all the other components.

As for the capacitor (C_{UT}), having a maximum applicable voltage of 700 V, the comparison method was used, like the one shown in [45] and [46]. A reference capacitor (C_{REF}), calibrated at INRIM, having a maximum applicable voltage of 34 kV is used. The same voltage is applied to C_{UT} and C_{REF}; their currents are measured through two 8.5 digit digital multimeters fluke 8508, calibrated at INRIM. Since the applied voltages are the same, the ratio of the measured currents depends on the ratio of the capacitances. From the knowledge of the voltage dependence of C_{REF} (measured at INRIM), the voltage dependence of C_{UT} is measured.

Various waveforms are used: 1) a 50-Hz sine wave with amplitude from 100 to 700 V; 2) a waveform with a fixed amplitude of 600 V composed by a 50-Hz fundamental tone and a 150 Hz and 30% harmonic tone with variable phase; and 3) a waveform with amplitude from 100 to 700 V composed by a 50 Hz fundamental tone, a 10 kHz and 2% tone, a 50 kHz and 1.2% tone and a 150 kHz and 1% tone.

It is worth to underline that the used waveforms represent realistic power system waveforms and a wide variety of waveform amplitudes and shapes are involved.

The maximum measured variation of C_{UT} in all the tests is lower than 0.031%.

As regards the resistor (R_{UT}), subjected to a maximum voltage of 20 V (when 3.6 kV is applied to HFRD), the resistance was measured by using two 8.5 digit digital multimeters fluke 8508, one as voltmeter and one as ammeter. Various waveforms are used: 1) a 50 Hz sine wave; 2) a10 kHz sine wave; 3) a 150 kHz sine wave; and 4) a waveform composed by a 50 Hz tone, a 10 kHz and 2% tone, a 50 kHz and 1.2% tone, a 150 kHz and 1% tone. The RMS amplitudes are in the range [1], [20] V.

The maximum measured variation of R_{UT} in all the tests is lower than 0.032%.

These effects are treated as an uncertainty source and included in the uncertainty of $\dot{G}_{\mathrm{HFRD}}$ in Section IV-D.

D. Uncertainty Associated With HFRD

Four uncertainty sources have been identified for HFRD SF and phase error: 1) the contribution of DAQ channels (coming from INRIM calibration); 2) variation of the frequency behavior with the input voltage amplitude (see Section IV-B); 3) the contribution of the nonlinear parasitic effects of HFRD resistors and capacitors (see Section IV-C); and 4) a contribution associated with repeatability and stability (evaluated through a type A approach [51]). The DAQ contribution is negligible compared to the other three. As regards the input voltage contribution, it is evaluated by accounting the maximum SF and phase error deviations (see Fig. 6). Similarly, the contribution of the nonlinear parasitic effects is evaluated by accounting the deviations measured in Section IV-C. The combined standard uncertainty on HFRD SF (phase error) goes from 600 μV/V (630 μrad) at 9 kHz to 7.0 mV/V (6 mrad) at 150 kHz.

V. Frequency Behavior of a VT: Measurement Model and Associated Uncertainty Budget

This section discusses the measurement model and the associated uncertainty related to the evaluation of the frequency behavior of a VT. Referring to the measurement architecture of

TABLE III
UNCERTAINTY BUDGET OF u_ϵ (μV/V) AND $u_{\Delta\phi}$ (μrad)

Source	Frequency (kHz)									
	0.05		9		50		100		150	
	u_ϵ (μV/V)	$u_{\Delta\phi}$ (μrad)	u_ϵ (μV/V)	$u_{\Delta\phi}$ (μrad)	u_ϵ (μV/V)	$u_{\Delta\phi}$ (μrad)	u_ϵ (μV/V)	$u_{\Delta\phi}$ (μrad)	u_ϵ (μV/V)	$u_{\Delta\phi}$ (μrad)
$\dot{G}_{LFRD}$	50	50	-	-	-	-	-	-	-	-
$\dot{G}_{HFRD}$	-	-	600	630	1500	2100	5000	4000	7000	6000
$\dot{G}_{LVD}$	50	50	200	150	350	150	1300	350	1000	350
$\dot{K}_{acq,jk}$	40	40	40	40	120	120	400	400	400	400
Repeatability and Stability	10	10	30	50	60	150	100	300	200	300
u_c	82	82	630	650	1600	2100	5200	4000	7100	6000
U_c (95 %)	160	160	1300	1300	3200	4200	10000	8000	14000	12000

Fig. 1(a), it is possible to express the complex gains of a DUT at fundamental frequency ($\dot{G}_{\mathrm{DUT,LF}}$) and at high frequency ($\dot{G}_{\mathrm{DUT,HF}}$), respectively, as in the following equation:

$$\dot{G}_{\mathrm{DUT,LF}} = \frac{\bar{V}_{ch3}}{\bar{V}_{ch1}} \frac{\dot{G}_{\mathrm{LFRD}}}{\dot{G}_{\mathrm{LVD}}} \dot{K}_{acq,31} \tag{5}$$

$$\dot{G}_{\mathrm{DUT,HF}} = \frac{\bar{V}_{ch3}}{\bar{V}_{ch2}} \frac{\dot{G}_{\mathrm{HFRD}}}{\dot{G}_{\mathrm{LVD}}} \dot{K}_{acq,32} \tag{6}$$

where

- $\bar{V}_{chX}$ is the phasor of the voltage acquired by the channel X of the DAQ;
- $\dot{G}_{\mathrm{LFRD}}$ is the complex gain of LFRD;
- $\dot{G}_{\mathrm{HFRD}}$ is the complex gain of HFRD obtained combining (3) and (4), $\dot{G}_{\mathrm{HFRD}} = (1/\mathrm{SF}_R)e^{j\Delta\varphi_R}$;
- $\dot{G}_{\mathrm{LVD}}$ is the complex gain of the LVD (it is present only in the case of inductive VTs or for any DUT with voltage output greater than the maximum input voltage of DAQ);
- $\dot{K}_{acq,jk}$ is the complex ratio between the gain of DAQ channel j and the DAQ channel k.

All the complex gains of (5) and (6) represent systematic deviations that are evaluated and compensated. The values of $\dot{G}_{\mathrm{LFRD}}$, $\dot{G}_{\mathrm{LVD}}$ and $\dot{K}_{acq,jk}$ and the associated uncertainties are obtained by the INRIM calibration (see Section III-A). The calibration of HFRD ($\dot{G}_{\mathrm{HFRD}}$) has been discussed in Section IV.

Table III reports, for each row, the uncertainty values, associated with a specific source, at various frequencies. Note that the contribution associated with $\dot{G}_{\mathrm{LFRD}}$ is present only in the first column because measurement model (5) applies only at 50 Hz. Repeatability and stability (evaluated through a type A approach [51]) on the complex ratios $\bar{V}_{chj}/\bar{V}_{chk}$ are also reported.

The last two rows of Table III report, respectively, the combined standard (u_c) and the expanded (U_c, level of confidence 95%) uncertainties associated with $\dot{G}_{\mathrm{DUT}}$. It can be noted that, especially at the higher frequencies, $\dot{G}_{\mathrm{HFRD}}$ is the main source of uncertainty. This is due to the effect of parasitic parameters, which becomes relevant at higher frequency and worsens the measurement repeatability, increasing, in turn, the uncertainty.

TABLE IV
RATED CHARACTERISTICS OF THE ANALYZED VTS

	Rated primary voltage (kV)	Rated secondary voltage (V)	Rated Burden (VA)	Accuracy class
LPVT	3	3	5	0.5
Inductive VT	3	100	20	0.5

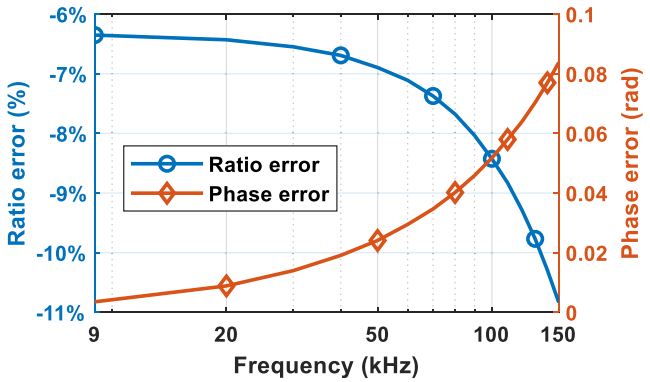

Fig. 7. Ratio and phase errors versus frequency for the LPVT.

VI. FREQUENCY CHARACTERIZATION OF COMMERCIAL VOLTAGE TRANSFORMERS

As an application of the realized measurement setup, the frequency characterization of two commercial VTs, a LPVT and an inductive VT was performed. the VTs' main features are summarized in Table IV.

The ratio and the phase errors of the VTs under test are measured as in (7) and in (8), respectively,

$$\varepsilon(f) = \frac{k_\mathrm{r} \cdot V_\mathrm{s}(f)}{V_\mathrm{p}(f)} - 1 \tag{7}$$

$$\Delta\varphi(f) = \varphi_s(f) - \varphi_p(f) \tag{8}$$

where $k_\mathrm{r} = V_{\mathrm{p,r}}/V_{\mathrm{s,r}}$ is the rated transformation ratio ($V_{\mathrm{p,r}}$ and $V_{\mathrm{s,r}}$ are the rated primary and secondary voltages).

The generated test waveforms are of FH1 type [50] and composed by the fundamental tone at 50 Hz and 3 kV, one frequency tone having frequency in the range [9, 150] kHz and amplitude equal to 2% of fundamental tone.

A. Characterization of LPVT

The ratio and phase errors of the LPVT at 50 Hz are, respectively, 0.1% and 600 μrad. Fig. 7 shows the ratio and phase errors in the range [9, 150] kHz. It can be observed that the ratio error is within 10% up to 130 kHz and equal to 11% at 150 kHz. The phase error is within 0.1 rad up to 150 kHz. With reference to the accuracy classes extensions defined in [11], regarding the ratio error, it can be observed that the LPVT totally meets the requirements of WB1 and WB2, whereas it only partially satisfies the requirements of WB3 and completely misses the ones of WB4. As regards the phase error, the LPVT meets the requirements of all the accuracy class extension, as the phase error is within $5.0° = 0.087$ rad up to 150 kHz.

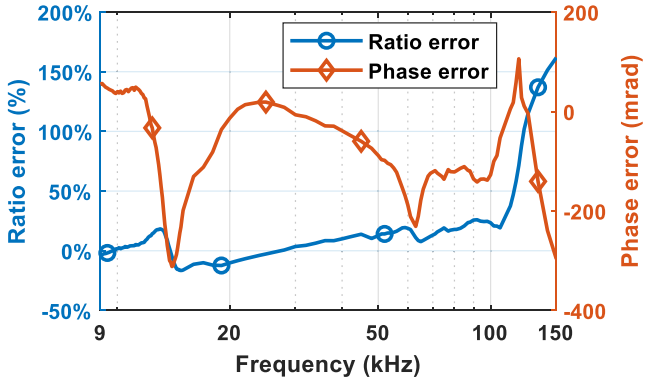

Fig. 8. Ratio and phase errors versus frequency for the inductive VT.

B. Characterization of Inductive VT

The ratio and phase errors of the inductive VT at 50 Hz are, respectively, 0.05% and 500 μrad. Fig. 8 shows the ratio and phase errors in the range [9, 150] kHz. It can be observed that the ratio error is within $\pm$20% up to 50 kHz. A first resonance occurs at about 12 kHz, whereas a second resonance, having a lower entity, at about 60 kHz. The last observable resonance occurs over 150 kHz. The phase error is within $\pm$0.4 rad up to 150 kHz. With reference to the accuracy class extensions defined in [11], regarding the ratio error, it can be observed that the inductive VT totally meets the requirements of WB1, whereas it completely misses the ones of WB2, WB3, and WB4. As regards the phase error, the inductive VT totally meets the requirements of WB1 and WB2, whereas it only partially satisfies the requirements of WB3 and WB4. The IEC 61869-1 ed.2 specifies that some extensions defined in [11] may not apply to some specific ITs. These results show that the extended accuracy class limit should not be applied to inductive VTs.

VII. Conclusion

This article has presented a novel generation and measurement setup for the frequency characterizations of MV VTs from 9 kHz up to 150 kHz. The proposed architecture represents an extension of the measurement setups commonly employed by NMIs to characterize VTs. The generation is obtained by a series connection between two generators, a high-frequency amplifier and a step-up transformer, used to generate the power frequency component at MV level. The measurement of the fundamental component and of the high frequency components are obtained through two different reference devices. A commercial divider is used as reference device for the measurement of the fundamental component. Instead, a new reference device, operating in the range [9, 150] kHz, is designed, realized, and characterized. The maximum uncertainty obtained with the proposed setup in the frequency range from 9 kHz up to 150 kHz lower than 1.4% and 12 mrad (level of confidence 95%) for the ratio and phase errors, respectively. In conclusion, the proposed generation and measurement setup allows for the characterization of inductive and LPVTs at power frequency and from 9 to 150 kHz with waveforms having amplitudes at MV level.

References

[1] *Power Line Communication Systems for Power Utility Applications*, Standard IEC 62488, 2012.
[2] P. Kotsampopoulos et al., "EMC issues in the interaction between smart meters and power-electronic interfaces," *IEEE Trans. Power Del.*, vol. 32, no. 2, pp. 822–831, Apr. 2017.
[3] S. K. Rönnberg, A. G. Castro, M. H. J. Bollen, A. Moreno-Munoz, and E. Romero-Cadaval, "Supraharmonics from power electronics converters," in *Proc. 9th Int. Conf. Compat. Power Electron. (CPE)*, Costa da Caparica, Portugal, Jun. 2015, pp. 539–544.
[4] K. Sarah et al., "On waveform distortion in the frequency range of 2 kHz-150 kHz—Review and research challenges," *Electric Power Syst. Res.*, vol. 150, pp. 1–10, Sep. 2017.
[5] Y. Xia, J. Roy, and R. Ayyanar, "Optimal variable switching frequency scheme to reduce loss of single-phase grid-connected inverter with unipolar and bipolar PWM," *IEEE J. Emerg. Sel. Topics Power Electron.*, vol. 9, no. 1, pp. 1013–1026, Feb. 2021.
[6] Z. Lu et al., "Medium voltage soft-switching DC/DC converter with series-connected SiC MOSFETs," *IEEE Trans. Power Electron.*, vol. 36, no. 2, pp. 1451–1462, Feb. 2021.
[7] E. O. A. Larsson, M. H. J. Bollen, M. G. Wahlberg, C. M. Lundmark, and S. K. Ronnberg, "Measurements of high-frequency (2–150 kHz) distortion in low-voltage networks," *IEEE Trans. Power Del.*, vol. 25, no. 3, pp. 1749–1757, Jul. 2010.
[8] V. Khokhlov, J. Meyer, A. Grevener, T. Busatto, and S. Rönnberg, "Comparison of measurement methods for the frequency range 2–150 kHz (Supraharmonics) based on the present standards framework," *IEEE Access*, vol. 8, pp. 77618–77630, 2020.
[9] S. T. Y. Alfalahi, "Supraharmonics in power grid: Identification, standards, and measurement techniques," *IEEE Access*, vol. 9, pp. 103677–103690, 2021.
[10] A. J. Collin, A. Delle Femine, C. Landi, R. Langella, M. Luiso, and A. Testa, "The role of supply conditions on the measurement of high-frequency emissions," *IEEE Trans. Instrum. Meas.*, vol. 69, no. 9, pp. 6667–6676, Sep. 2020.
[11] J. G. Wellings, "Instrument transformers," *Electron. Power*, vol. 13, no. 3, pp. 93–94, Mar. 1967.
[12] *Instrument Transformers—Part 1: General Requirements*, Standard IEC 61869-1, 2023.
[13] *EPM 22NRM06 ADMIT*. Accessed: Aug. 27, 2024. [Online]. Available: https://www.euramet.org/research-innovation/search-research-projects/details/project/characterisation-of-ac-and-dc-mv-instrument-transformers-in-extended-frequency-range-up-to-150-khz
[14] *EMPIR 17IND06 Future Grid II*. Accessed: Aug. 27, 2024. [Online]. Available: https://www.euramet.org/index.php?id=2008&tx_eurametctcp_project%5Bproject%5D=1533&tx_eurametctcp_project%5Baction%5D=show&tx_eurametctcp_project%5Bcontroller%5D=Project&cHash=01f79ce97b00442a96816a618d2a41cf
[15] *EMPIR 17IND06 Future Grid II Project*. Accessed: Aug. 27, 2024. [Online]. Available: https://projectsites.vtt.fi/sites/FutureGrid2
[16] *EMPIR 19NRM05 IT4PQ*. Accessed: Aug. 27, 2024. [Online]. Available: https://www.euramet.org/smart-electricity-grids/projects/details/project/measurement-methods-and-test-procedures-for-assessing-accuracy-of-instrument-transformers-for-power
[17] *EMPIR 19NRM05 IT4PQ Project*. Accessed: Aug. 27, 2024. [Online]. Available: https://www.it4pq.eu/
[18] W. Yan, I. Dewayalage, I. Budovsky, F. Emms, and Y. Li, "A reference measurement system for calibration of high-voltage transducers at frequencies up to 10 kHz," in *Proc. IEEE 13th Int. Workshop Appl. Meas. for Power Syst. (AMPS)*, Bern, Switzerland, Sep. 2023, pp. 1–6, doi: 10.1109/amps59207.2023.10297239.
[19] M. Kaczmarek and E. Stano, "Measuring system for testing the transformation accuracy of harmonics of distorted voltage by medium voltage instrument transformers," *Measurement*, vol. 181, Aug. 2021, Art. no. 109628, doi: 10.1016/j.measurement.2021.109628.
[20] M. Kaczmarek, "The effect of distorted input voltage harmonics rms values on the frequency characteristics of ratio error and phase displacement of a wideband voltage divider," *Electric Power Syst. Res.*, vol. 167, pp. 1–8, Feb. 2019, doi: 10.1016/j.epsr.2018.10.013.
[21] M. Klatt, J. Meyer, M. Elst, and P. Schegner, "Frequency responses of MV voltage transformers in the range of 50 Hz to 10 kHz," in *Proc. 14th Int. Conf. Harmon. Quality Power*, Bergamo, Italy, Sep. 2010, pp. 1–6.
[22] G. Crotti et al., "Characterization of voltage transformers for MV applications up to 150 kHz—A preliminary study," in *Proc. IEEE 13th Int. Workshop Appl. Meas. Power Syst. (AMPS)*, Bern, Switzerland, Sep. 2023, pp. 1–5, doi: 10.1109/amps59207.2023.10297174.

[23] G. D'Avanzo et al., "Theory and experimental validation of two techniques for compensating VT nonlinearities," *IEEE Trans. Instrum. Meas.*, vol. 71, pp. 1–12, 2022.
[24] G. Crotti, G. D'Avanzo, P. S. Letizia, and M. Luiso, "The use of voltage transformers for the measurement of power system subharmonics in compliance with international standards," *IEEE Trans. Instrum. Meas.*, vol. 71, pp. 1–12, 2022.
[25] E. Mohns, J. Chunyang, H. Badura, and P. Raether, "A fundamental step-up method for standard voltage transformers based on an active capacitive high-voltage divider," *IEEE Trans. Instrum. Meas.*, vol. 68, no. 6, pp. 2121–2128, Jun. 2019.
[26] M. Faifer, A. Ferrero, C. Laurano, R. Ottoboni, S. Toscani, and M. Zanoni, "An innovative approach to express uncertainty introduced by voltage transformers," *IEEE Trans. Instrum. Meas.*, vol. 69, no. 9, pp. 6696–6703, Sep. 2020.
[27] A. Mingotti, L. Peretto, and R. Tinarelli, "Effects of multiple influence quantities on rogowski-coil-type current transformers," *IEEE Trans. Instrum. Meas.*, vol. 69, no. 7, pp. 4827–4834, Jul. 2020.
[28] G. Crotti et al., "Measurement of dynamic voltage variation effect on instrument transformers for power grid applications," in *Proc. IEEE Int. Instrum. Meas. Technol. Conf. (IMTC)*, Dubrovnik, Croatia, May 2020, pp. 1–6, doi: 10.1109/I2MTC43012.2020.9129354.
[29] R. Stiegler and J. Meyer, "Impact of external influences on the frequency dependent transfer ratio of resin cast MV voltage instrument transformers," in *Proc. 20th Int. Conf. Harmon. Quality Power (ICHQP)*, Naples, Italy, May 2022, pp. 1–6.
[30] J. Hällström et al., "Performance of a modular wideband HVDC reference divider for voltages up to 1000 kV," *IEEE Trans. Instrum. Meas.*, vol. 64, no. 6, pp. 1390–1397, Jun. 2015.
[31] G. Crotti, G. D'Avanzo, D. Giordano, P. S. Letizia, and M. Luiso, "Extended SINDICOMP: Characterizing MV voltage transformers with sine waves," *Energies*, vol. 14, no. 6, p. 1715, 2021.
[32] G. Crotti, D. Giordano, G. D'Avanzo, P. S. Letizia, and M. Luiso, "A new industry-oriented technique for the wideband characterization of voltage transformers," *Measurement*, vol. 182, 2021, Art. no. 109674.
[33] G. Crotti, G. D'Avanzo, P. S. Letizia, and M. Luiso, "Measuring harmonics with inductive voltage transformers in presence of subharmonics," *IEEE Trans. Instrum. Meas.*, vol. 70, pp. 1–13, 2021.
[34] A. Mingotti, F. Costa, L. Peretto, and R. Tinarelli, "Effect of proximity, burden, and position on the power quality accuracy performance of Rogowski coils," *Sensors*, vol. 22, no. 1, p. 397, Jan. 2022.
[35] A. Mingotti, F. Costa, L. Peretto, and R. Tinarelli, "Accuracy type test for Rogowski coils subjected to distorted signals, temperature, humidity, and position variations," *Sensors*, vol. 22, no. 4, p. 1397, Feb. 2022.
[36] P. S. Letizia, D. Signorino, and G. Crotti, "Impact of DC transient disturbances on harmonic performance of voltage transformers for AC railway applications," *Sensors*, vol. 22, no. 6, p. 2270, Mar. 2022.
[37] G. Crotti et al., "How instrument transformers influence power quality measurements: A proposal of accuracy verification tests," *Sensors*, vol. 22, no. 15, p. 5847, Aug. 2022.
[38] C. Buchhagen, M. Fischer, L. Hofmann, and H. Däumling, "Metrological determination of the frequency response of inductive voltage transformers up to 20 kHz," in *Proc. IEEE Power Energy Soc. Gen. Meeting*, Vancouver, BC, Canada, Jul. 2013, pp. 1–5, doi: 10.1109/PESMG.2013.6672835.
[39] G. Crotti, G. D'Avanzo, C. Landi, P. S. Letizia, and M. Luiso, "Evaluation of voltage transformers' accuracy in harmonic and interharmonic measurement," *IEEE Open J. Instrum. Meas.*, vol. 1, pp. 1–10, 2022.
[40] A. Mingotti, C. Betti, L. Peretto, and R. Tinarelli, "Simplified and low-cost characterization of medium-voltage low-power voltage transformers in the power quality frequency range," *Sensors*, vol. 22, no. 6, p. 2274, Mar. 2022.
[41] A. Ghaderi, A. Mingotti, L. Peretto, and R. Tinarelli, "Low-power voltage transformer smart frequency modeling and output prediction up to 2.5 kHz, using sinc-response approach," *Sensors*, vol. 20, no. 17, p. 4889, Aug. 2020.
[42] L. J. Giakoletto, *Electronic Designer's Handbook*. New York, NY, USA: McGraw-Hill, 1977.
[43] K. C. Kao, *Dielectric Phenomena in Solids*, 1st ed. Amsterdam, The Netherlands: Elsevier, Mar. 2004.
[44] E. Jaynes, "Nonlinear dielectric materials," *Proc. IRE*, vol. 43, no. 12, pp. 1733–1737, 1955.
[45] D. Slomovitz, M. Brehm, D. Izquierdo, C. Faverio, J. L. Casais, and M. H. Cazabat, "Determination of voltage dependence in high-voltage standard capacitors," *IEEE Trans. Instrum. Meas.*, vol. 68, no. 6, pp. 2136–2143, Jun. 2019.
[46] Y. Pan et al., "Investigation on the voltage dependence of compressed-gas-insulated capacitors up to 400 kV by improved voltage-doubling method," *IEEE Trans. Instrum. Meas.*, vol. 71, pp. 1–7, 2022.
[47] G. Crotti et al., "Frequency compliance of MV voltage sensors for smart grid application," *IEEE Sensors J.*, vol. 17, no. 23, pp. 7621–7629, Dec. 2017.
[48] *Electromagnetic Compatibility (EMC)—Part 3–40: Testing and Measurement Techniques—Power Quality Measurement Methods*, Standard IEC 61000-4-30, 2015.
[49] *Electromagnetic Compatibility (EMC)—Part 4–7: Testing and Measurement Techniques—General Guide on Harmonics and Interharmonics Measurements and Instrumentation, for Power Supply Systems and Equipment Connected Thereto*, Standard IEC 61000-4-7, 2008.
[50] A. Cataliotti et al., "Compensation of nonlinearity of voltage and current instrument transformers," *IEEE Trans. Instrum. Meas.*, vol. 68, no. 5, pp. 1322–1332, May 2019.
[51] *Guide to the Expression of Uncertainty in Measurement*, Int. Org. Standardization, Supported By BIPM, IEC, IFCC, ISOIUPAC, IUPAP and OIML, Geneva, Switzerland, 2008.

Gabriella Crotti received the degree (cum laude) in physics from the University of Turin, Turin, Italy, in 1986.

Since then, she has been with the Istituto Nazionale di Ricerca. Metrologica (INRIM), Turin, where she currently works as the Director Technologist of the Electric and Electromagnetic Field and System Sector. She was the Leader of the EMPIR project 19NRM05 IT4PQ. Her research interests include development and characterization of references and techniques for voltage and current measurements in high and medium voltage grids and on the traceability of electric and magnetic field measurements at low and intermediate frequency.

Giovanni D'Avanzo received the master's degree in electronic engineering and the Ph.D. degree in electrical energy conversion from the University of Campania "Luigi Vanvitelli," Aversa, Italy, in 2019 and 2023, respectively.

He is currently with Ricerca sul Sistema Energetico S.p.A., Milan, Italy, where he is working on various European metrology research projects. His research interests include the characterization of instrument transformers under power quality phenomena, the development of smart meters, and measurement systems.

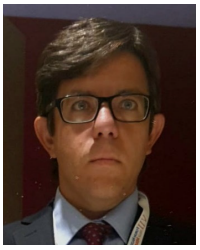

Antonio Delle Femine (Member, IEEE) received the M.Sc. degree (summa cum laude) in electronic engineering and the Ph.D. degree in electrical energy conversion from the University of Campania, Aversa, Italy, in 2005 and 2008, respectively.

From 2008 to 2017, he was a freelancer with many national and international companies. He worked as Software and Hardware Engineer (Ditron S.r.l., Italy), Senior Embedded Firmware Engineer (G-LAB gmbH, Switzerland). He was involved in the design of many products for both industrial and consumer electronics: he worked on fleet monitoring, thermal printers, electronic scales and cash registers, distributed monitoring systems for PV plants, Hi-Fi radios and home appliances, automatic end-of-line testing, augmented reality devices, and radioactivity measurement instrumentation (in collaboration with the Institute of Nuclear Physics, INFN, Naples, Italy). Since 2018, he has been a Researcher with the University of Campania. His main scientific interests include power measurement theory, the design, implementation and characterization of digital-measurement instrumentation and automatic measurement systems, radioactivity measurements, wearable sensors, and physiological measurements.

Dr. Femine is a member of the Instrumentation and Measurement Society.

Daniele Gallo (Member, IEEE) received the Laurea degree in electronic engineering and the Ph.D. degree in electrical energy conversion from the University of Campania "Luigi Vanvitelli" (formerly Second University of Naples), Aversa, Italy, in 1999 and 2003, respectively.

He is currently a Full Professor with the University of Campania "Luigi Vanvitelli." He has authored numerous scientific papers and had the responsibility of different research projects. His main scientific interests are: DC and AC Power quality analysis; power and energy measurement in nonsinusoidal conditions; design, implementation and characterization of measurement systems for electrical power system; design and implementation of smart meter for smart grid application; electrical transducer characterization.

Domenico Giordano (Member, IEEE) received the Ph.D. degree in electrical engineering from the Politecnico di Turin, Turin, Italy, in May 2007.

Since December 1, 2010, he has been a Researcher, permanent position with the Quality of Life Division, Istituto Nazionale di Ricerca Metrologica (INRIM), Turin. He is currently coordinating the European EPM project 22NRM04 e-TRENY. His research activities are focused on the development and characterization of systems and voltage/current transducers for calibration and power quality measurements on medium voltage grids and on railway supply systems, on the calibration of energy meters for onboard train installation, and on the study of ferroresonance phenomena. Moreover, he is involved in the development of generation and measurement systems of electromagnetic fields for calibration and dosimetric purposes.

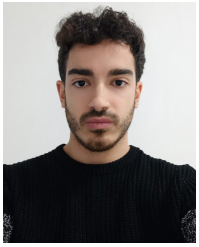

Claudio Iodice (Graduate Student Member, IEEE) was born in Naples, Italy, in 1997. He received the M.Sc. degree (summa cum laude) in aerospace engineering from the University of Campania "Luigi Vanvitelli," Aversa, Italy, where he is currently pursuing the Ph.D. degree in energy conversion.

His main scientific interests are calibration of instrument transformers, measurement systems for e-mobility, and control and optimization algorithms for aerospace applications.

Carmine Landi (Senior Member, IEEE) was born in Salerno, Italy, in 1955. He received the Laurea degree in electrical engineering from the University of Naples, Naples, Italy, in 1981.

He was an Assistant Professor of electrical measurement from the University of Naples "Federico II," Naples, from 1982 to 1992. He was an Associate Professor in electrical and electronic measurements with the University of L'Aquila, L'Aquila, Italy, from 1992 to 1999. He has been a Full Professor with the University of Campania "Luigi Vanvitelli" (formerly Second University of Naples), Aversa, Italy, since 1999. His main scientific interests include related to the setup of digital measurement instrumentation, the automatic testing of electrical machines such as asynchronous motors and power transformers, measurement techniques for the characterization of digital communication devices, and the use of digital signal processors for real-time measurements. He has authored almost 200 international papers in the field of real-time measurement apparatus, automated test equipment, high precision power measurement, and power quality measurement.

Palma S. Letizia received the M.Sc. degree (summa cum laude) in power electronic engineering from the University of Campania "Luigi Vanvitelli," Aversa, Italy, in 2018, and the Ph.D. degree in metrology from the Politecnico di Turin, Turin, Italy, in 2022.

Since 2022, she has been as a Researcher with the Istituto Nazionale di Ricerca Metrologica (INRIM), Turin. Her main scientific interests include metrology applied to power grids, particularly in the development of new procedures and reference sensors for power quality and phasor measurement unit applications.

Mario Luiso (Member, IEEE) was born in Naples, Italy, in July 6, in 1981. He received the Laurea degree (summa cum laude) in electronic engineering and the Ph.D. degree in electrical energy conversion from the University of Campania "Luigi Vanvitelli," Aversa, Italy, in 2005 and 2007, respectively.

He currently is an Associate Professor with the Department Engineering, University of Campania "Luigi Vanvitelli." He has authored and coauthored more than 200 articles published in books, scientific journals, and conference proceedings. His main scientific interests include related to the development of innovative methods, sensors and instrumentation for power system measurements, in particular power quality, calibration of instrument transformers, phasor measurement units, and smart meters.

Dr. Luiso is a member of the IEEE Instrumentation and Measurement Society.

Paolo Mazza (Member, IEEE) received the M.Sc. degree in electrical engineering from the Politecnico di Milan, Milan, Italy, in 1997.

In 1997, he joined CESI S.p.A., Milan, where he was involved in developing methodologies and facilities aimed at aging tests of HV and MV components. Since 2006, he has been with Ricerca sul Sistema Energetico (RSE) S.p.A, Milan, where he has carried out many research activities in the field of instrument transformers and power and energy measurements. He is currently the Head of the Measurements and Diagnostics for Power Systems Unit and of the RSE Accredited Laboratory LAT n. 057, for the calibration of HV impulse measurement systems and of voltage and current transformers.

Open Access funding provided by 'Università degli Studi della Campania "Luigi Vanvitelli"'
within the CRUI CARE Agreement